Seismic reliability assessment of base-isolated structures using artificial neural network: operation failure of sensitive equipment

Hesamaldin Moeindarbari[a] and Touraj Taghikhany[*]

Civil and Environmental Engineering Department Amirkabir University of Technology, Tehran, Iran

Abstract.　The design of seismically isolated structures considering the stochastic nature of excitations, base isolators' design parameters, and superstructure properties requires robust reliability analysis methods to calculate the failure probability of the entire system. Here, by applying artificial neural networks, we proposed a robust technique to accelerate the estimation of failure probability of equipped isolated structures. A three-story isolated building with susceptible facilities is considered as the analytical model to evaluate our technique. First, we employed a sensitivity analysis method to identify the critical sources of uncertainty. Next, we calculated the probability of failure for a particular set of random variables, performing Monte Carlo simulations based on the dynamic nonlinear time-history analysis. Finally, using a set of designed neural networks as a surrogate model for the structural analysis, we assessed once again the probability of the failure. Comparing the obtained results demonstrates that the surrogate model can attain precise estimations of the probability of failure. Moreover, our proposed approach significantly increases the computational efficiency corresponding to the dynamic time-history analysis of the structure.

Keywords:　seismic reliability; neural network; base isolation; friction pendulum; sensitivity analysis; equipment protection

1. Introduction

Base isolation has attracted much interest among engineers in recent decades as a technology for providing seismic protection to building structures. The use of isolation systems at the base of a structure elongates its period of vibration and dissipates the seismic input energy, thereby allowing better control of the structural response.

Among the different types of implemented isolators, friction pendulum systems (FPSs) have become widespread since 1990 (Zayas *et al*. 1990). FPS consists of a concave spherical sliding surface and a slider, forming an innovative bearing that achieves damping through friction. Many studies have been conducted on this type of isolation systems and other developed generations of FPS (Moeindarbari *et al*. 2014, Moeindarbari and Taghikhany 2014, Shahbazi and Taghikhany 2017).

Castaldo and Tubaldi analysed the influence of FPS isolator properties on the seismic performance of base-isolated building frames. The uncertainty in the seismic input was taken into account by only considering a set of natural records with different characteristics scaled to increasing intensity levels (Castaldo and Tubaldi 2015). Bucher discussed the analysis of all types of friction pendulum isolators and compared their behaviour to the

isolation capacity and device displacements (Bucher 2015). These studies were developed mainly through deterministic analyses, whereas the isolation system characteristics, structural system properties, earthquake characteristics, and device properties contain inherent uncertainties.

The stochastic nature of variables such as input ground motion motivates the use of probabilistic analysis in structural dynamics, structural reliability methods, and reliability-based analysis (Enevoldsen and Sørensen 1994, Lin and Cai 1995, Ayyub and McCuen 2011). Several studies have thus focused on the design analysis of isolated structures by considering uncertainties in the structural, base-isolation, and ground-motion characteristics (Pourgharibshahi and Taghikhany 2012). Su and Ahmadi (1988) studied the responses of a rigid structure with a frictional base isolation system subjected to randomly generated horizontal-vertical earthquake excitations. Constantinou and Papageorgiou (1990) discussed the stochastic response of practical sliding isolation systems. Alhan and Gavin (2005) studied the reliability requirements of isolation-system components to protect critical equipment from earthquake hazards. They considered a four-story structure representing a sensitive facility on an isolated raised floor at the second level of the building. The stochastic seismic response analysis and reliability evaluation of the base-isolated structures were conducted by combining a physical stochastic ground-motion model and the probability density evolution method by Chen *et al*. in 2007 (Chen *et al*. 2007). They concluded that the response and earthquake action on the superstructure could be reduced by one degree of intensity, relative to a fixed-based structure. The investigations showed that the stochastic

---

*Corresponding author, Assistant Professor
 E-mail: ttaghikhany@aut.ac.ir
[a]Ph.D. Student
 E-mail: hessammoeen@aut.ac.ir

seismic response analysis and reliability assessment could provide indices that allow more objectivity in decision making than the few selected deterministic ground motions commonly employed in practice. Xiao *et al.* (Zou *et al.* 2010) in 2010 presented a useful numerical reliability-based optimisation technique for the design of base-isolated concrete building structures under spectrum loading. Huang and Ren presented a dynamic reliability-based optimisation technique for the seismic design of base-isolated structures. Analytical solutions of stochastic seismic response under the Kanai-Tajimi spectrum loading were obtained applying on a 3-story isolated building (Huang and Ren 2011). Taflanidis and Jia proposed a versatile, simulation-based framework for risk assessment and probabilistic sensitivity analysis of base-isolated structures. A sampling-based approach was also introduced for establishing a probabilistic sensitivity analysis to quantify the significance of each uncertain model parameter for affecting the overall risk (Taflanidis and Jia 2011). Jia *et al.* (2014) optimised the floor isolation system based on reliability criteria, where the reliability of the system was quantified, by stochastic simulations, in terms of the plausibility that the acceleration of the protected contents will not exceed an acceptable performance limit. In 2014 Palazzo *et al.* evaluated the seismic reliability of a base-isolated structure with FPS considering both isolator properties and earthquake key features as random variables. They used Latin hypercube sampling (LHS) as the sampling method for Monte Carlo simulations (Palazzo *et al.* 2014).

Simulation-based methods achieve the best estimates in the reliability analysis of the isolated structure via a dynamic time-history model of the isolated structure. Simulation-based methods for reliability analysis are useful tools for calculating the probability of failure (P_f) or reliability index (β) of an isolated structure subjected to random earthquake excitations (Alhan and Gavin 2005). An important issue in such methods is the computation cost. For complex systems where the derivation of joint probability-distribution functions is complicated, the probability of failure is evaluated by Monte Carlo simulations (MCSs). In fact, P_f is the ratio of the number of realisations with non-positive limit states to the total number of simulations. The required number of simulations for complex dynamics is often too large to complete over reasonable time frames. Several modified MCS methods were therefore developed to reduce the size of calculations. Various sampling variance-reduction techniques were developed to improve computation efficiency by minimising the sample size and reducing the statistical error inherent in MCSs. These techniques include importance sampling, adaptive sampling, stratified sampling, Latin-hypercube sampling, the antithetic variate technique, the conditional expectation technique, average sampling, and asymptotic sampling (Papadrakakis *et al.* 2004, Iman 2008, Bucher 2009).

Other efficient newly developed methods for simulation-based reliability analyses, which can significantly reduce computation size, involve estimating the limit states using the response surface (Gosavi 2014, Dai *et al.* 2015). The former methods called response-

surface methods (RSMs) are used primarily in reliability-based design optimisation (RBDO) (Gosavi 2003). One of the most appropriate tools in RSM is the artificial neural network (ANN) and its recent variants such as wavelet neural networks (Farooq Anjum *et al.* 1997, Desai *et al.* 2008). Kerh and Ting used a back-propagation neural network model, to estimate peak ground acceleration at ten train stations along the high-speed rail system in Taiwan (Kerh and Ting 2005). Liu *et al.* used neural networks to train a classifier for damage diagnosis of structures (Liu *et al.* 2011). Papadrakakis and Lagaros (2002) examined the application of neural networks (NNs) to the reliability-based structural optimisation of large-scale structural systems. The failure of the structural system in that study was associated with plastic collapse. Other studies demonstrated the efficiency of neural networks as a tool for estimating the limit-state function (Gomes and Awruch 2004). Adeli and Jiang presented a new dynamic time-delay fuzzy wavelet neural network model for nonparametric identification of structures using the nonlinear autoregressive moving average with exogenous inputs approach (Adeli and Jiang 2006).

The present study deals with the seismic reliability analysis of a base-isolated structure using MCSs. Although the Monte Carlo simulations for the reliability analysis of a single specific isolated structure does not impose high calculation cost, in the optimal reliability-based design of an isolated structure, the failure probability should be calculated for several times due to the properties variation of the supposed system. Thus we present two methods aimed at decreasing the computation cost of reliability analysis: (I) by exploiting NN efficiency as a meta-model to predict the maximum structural responses; and (II) by reducing the number of uncertain variables using a recent sensitivity analysis to ignore the uncertainty of some input variables of the meta-model. The NN estimates are used instead of direct time-history analysis in the Monte Carlo simulations as a surrogate model for calculating the probability of failure. Applying sensitivity analysis beside NN improves the efficiency of the NN design procedure.

The input variables of the surrogate model are the design variables of the isolated structure beside the uncertain variables of the entire analytical model.

Protecting delicate facilities in a structure as one of the applications of seismic base isolation is chosen for the desired performance of the structure in this paper. Therefore, as an innovative study, the limit state is defined by the maximum acceleration response of the floors. The reliability of the structure is computed using the estimations of the limit state by the designed NNs to show the efficiency of the introduced method. Accordingly, the results obtained from the evaluations of NN are compared with the results from the direct time-history analysis.

2. The selected model and assumptions

2.1 Superstructure
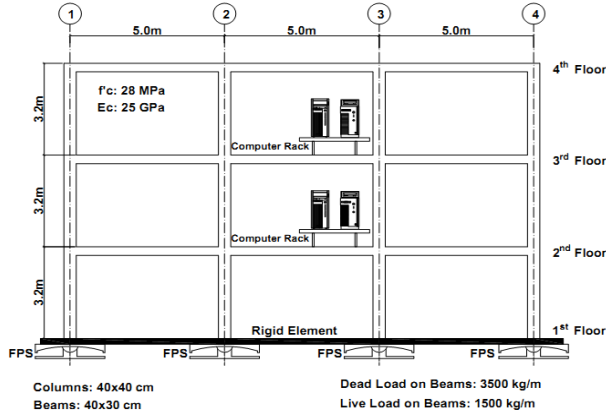
In this study, an isolated two-dimensional, three-story

Fig. 1 The two-dimensional three-story concrete frame modelled for the simulations

Fig. 2 FP Bearing, deformed shape and the slider free body diagram

concrete frame (see Fig. 1) is purposed for stochastic analyses. The sensitive computer servers are installed on the second and third floors of the supposed structure.

The structure is subjected to the ground motions generated randomly through the combination of parametric or functional descriptions of the amplitude spectrum with a random phase spectrum as discussed later.

At first, all the loads and resistant parameters of the structure assumed as random variables; however, to reduce the input parameters of the surrogate model, only essential variables are selected as random by using sensitivity analysis.

For the probability of failure, the limit state is defined using a function to determine the case where the facility floor accelerations reach a 100 milli-g acceleration level. Acceleration levels in the range of 100–200 milli-g are specified by computer producers for sensitive computers as the limit where they fail to operate (Alhan and Gavin 2005). Supposing a floor acceleration threshold a_t the limit state function can be formally stated with

$$g(X) = a_t - MFA \tag{1}$$

MFA is the maximum floor acceleration of the story where the facility is installed. Then the probability of failure is defined as

$$P_f = P[g(X) \le 0] \tag{2}$$

2.2 Mechanical behaviour and design of FPS (Single-FP bearings)

Single-FP bearings are devices which support the vertical load and transmit horizontal loads in a predefined manner through an articulated slider which slides on a concave surface with a radius R and friction coefficient μ as indicated in Fig. 2.

The centre of the spherical concave plate follows a circular trajectory so that the motion is that of a pendulum having a length equal to the radius of curvature R. As shown in Fig. 2 the resisting force F has two components; the pendulum component and the friction component which are determined from the following equations
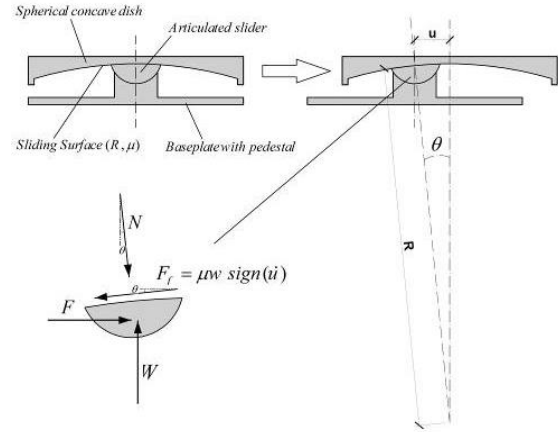
$$\left. \begin{array}{l} F - N\sin(\theta) - F_f \cos(\theta) = 0 \\ W - N\cos(\theta) - F_f \sin(\theta) = 0 \\ u = R\sin(\theta) \\ \cos(\theta) \gg 1 \end{array} \right\} \rho F = (\frac{W}{R})u + F_f \tag{3}$$

$$\rho F = (\frac{W}{R})u + \mu w\, sign(\ddot{u})$$

Where u is the horizontal displacement of the pivot point of the slider, *sign* denotes the signum function of the sliding velocity $\dot{u}$, R is the radius of curvature of the spherical surface, W is the contributing weight of superstructure on the bearing and μ is the coefficient of sliding friction. The magnitude of μ is a function of different parameters as; sliding velocity, vertical pressure, cycling and breakaway effects (Lomiento *et al.* 2013).

In this study only the dependency of the coefficient of friction to the velocity is considered which is given by the following equation (Constantinou *et al.* 1990, Mokha *et al.* 1990)

$$\mu = \mu_{max} - (\mu_{max} - \mu_{min})\exp(-a|\dot{u}|) \tag{4}$$

where μ_{max} is the friction coefficient due to high velocities, μ_{min} is the friction coefficient in the lowest (or negligible) velocities and *a is* the rate parameter that adjusts the speed of the transition of the friction coefficient between μ_{max} and μ_{min}.

The fundamental period of vibration of the system, T, related only to pendulum component, is independent of the mass of the structure and associated only with the radius of curvature of the spherical surface R.

$$T = 2\pi\sqrt{\frac{R}{g}} \tag{5}$$

To evaluate the efficiency of the proposed technique, we compared the results of the meta-model and the direct time-history analysis considering a specific base isolation system. So we designed an FPS for the supposed structure considering a desired effective isolated period T=2 second.

For the considered structure (Fig. 1), FPS is designed

based on the procedures proposed by Mayes and Naeim (2001). We computed the radius of curvature to be R=1 m from Eq. (5) considering an effective isolation period T=2 sec. Supposing Seismic Zone 4, Site Class D and Seismic Group 1 based on the NEHRP seismic provisions, Spectral Coefficients S_{M1} and S_{D1} would be 0.427 and 0.640 respectively. Assuming the target provided damping of the isolation system β_I=20% leads to numerical coefficient B_I=1.5. So the horizontal displacement capacity (D) can be computed by

$$D_M = (\frac{g}{4\pi^2})(\frac{S_{D1}T}{B_I}) = (\frac{9.81}{4\pi^2})(\frac{0.64 \times 2}{1.5}) = 0.212\,m \qquad (6)$$

Then the coefficient of friction would be approximately μ=0.11 from the following equation

$$\beta_I = \frac{2}{\pi}\frac{\mu}{\mu + D_M / R} \qquad (7)$$

So the design procedure for the isolated structure leads to the friction pendulum system having a concave surface with a one-meter radius of curvature and a friction coefficient equal to 0.11.

3. Input ground motion

There is two approaches available for time-history dynamic analysis of structures subjected to earthquakes: (1) dynamic response-history analysis using a set of recorded ground motion time-histories and (2) stochastic dynamic analysis employing a set of generated stochastic ground motions. Artificial ground motions are created through the combination of parametric or functional descriptions of the amplitude spectrum with a random phase spectrum. They randomly cover the complete range of the characteristics of ground motions with different duration, magnitude and the distance from the source. Accordingly, for simulation-based reliability analysis of the isolated structure, the best method is applying random excitation using artificial earthquake ground motions. This means of simulating ground motions is often called "Stochastic Method".

Herein the proposed point-source stochastic method by Boore (2003) is applied considering some modifications. In this method, the correlation between random variables is not observed. So the results can be improved using another technique that examines the correlation between the random variables.

Regarding the aim of this research, the parametric descriptions of the ground motion (such as the earthquake magnitude and the distance from the source) considered being random variables.

In this method the total spectrum of the motion at a site ($Y(M_0,R,f)$) is broken into contributions from earthquake source (E), path (P), site (G) and instrument or type of motion (I), so that

$$Y(M_0,R,f) = E(M_0,f)P(R,f)G(f)I(f) \qquad (8)$$

The total spectrum would be a function of M instead of M_0, using the unit mapping between the moment magnitude (M) and seismic moment (M_0)

Table 1 Parameters of source spectrum (E) for AS00 model

Parameter	Value
Sa	$\dfrac{1-\varepsilon}{1+(f/f_a)^2} + \dfrac{\varepsilon}{1+(f/f_b)^2}$
Sb	1
$\log fa$	2.181-0.496M
$\log fb$	2.41-0.408M
$\log \varepsilon$	0.605 - 0.255M
$R_{\Theta\Phi}, V, F, \rho_s, \beta_s, R_0$	0.55, 0.707, 2.0, 2.8, 3.5, 1

$$M = \frac{2}{3}\log M_0 - 10.7 \qquad (9)$$

Here, each component of the Eq. (8) is discussed separately.

3.1 The source effect E (M0, f)

The source spectrum is given by the following equation

$$E(M_0,f) = C M_0 S_a(M_0,f)S_b(M_0,f) \qquad (10)$$

Where the constant C is given by

$$C = \frac{R_{\Theta\Phi}VF}{4\pi\rho_s\beta_s^3 R_0} \qquad (11)$$

$R_{\Theta\Phi}$ is the radiation pattern, V represents the partition of total shear-wave energy into horizontal components, F is the effect of the free surface, ρ_s and β_s are the density, and shear-wave velocity in the vicinity of the source and R_0 is a reference distance, usually set equal to 1 km. Regarding using of mixed units, if the ground motion is to be in cm and ρ_s, β_s, and R_0 are in units of gm/cc, km/s, and km, respectively, then C in Eq. (11) should be multiplied by the factor 10^{-20}.

S_a and S_b are components of displacement source spectrum that are a function of corner frequencies (f_a and f_b) and moment ratio (ε). Referring to the research by Atkinson and Silva (AS00 model) (Atkinson and Silva 2000) parameters for the source spectrum are gathered in Table 1.

3.2 The path effect P (R, f)

The next component that affects the spectrum of motion is radiation path. The following equation can give the effect of radiation path in motion spectrum

$$P(R,f) = Z(R)\exp\left[-\pi fR / Q(f)c_Q\right] \qquad (12)$$

Where the geometrical spreading function $Z(R)$ is given by

$$Z(R) = \begin{cases} \dfrac{1}{R} & ;R < 40 \\ \dfrac{1}{40}\left(\dfrac{40}{R}\right)^{0.5} & ;R \geq 40 \end{cases} \qquad (13)$$

R is the closest distances to the rupture surface that can be calculated, having the closest distance to the vertical projection of the rupture surface onto the ground surface (r)

Table 2 Parameters of path spectrum (P) for AS00 model

Parameter	Value
Q	$180f^{0.45}$
C_Q	3.5 km/s
R	$\sqrt{r^2 + h_d^2}$
h_d	$10^{0.15-0.05M}$
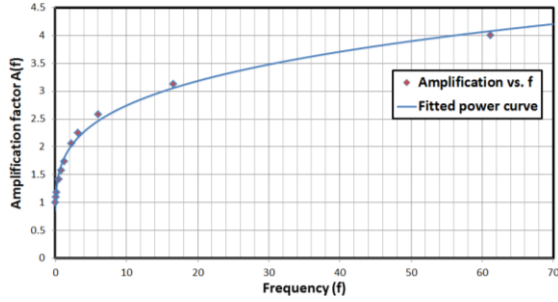
Fig. 3 Curve fitting for amplification factor $A(f)$

and hypocentral depth (h_d). Parameters for calculation of path spectrum are given by Table 2.

3.3 The site effect G (f)

Albeit the modification of seismic waves by local site conditions is part of the path effect, it would be convenient to separate the site and path effects due to the largely independent local site effects. In such case, the site spectrum (G) can be given by

$$G(f) = A(f)D(f) \tag{14}$$

Where $A(f)$ and $D(f)$ are the amplification and attenuation functions. $A(f)$ can be calculated using amplification factors proposed in a study by Boore and

Table 3 Parameters of temporal window function $w(t, \varepsilon_w, \eta, t_\eta)$ for AS00 model

Parameter	Value
ε_w	0.2
η	0.05
b	$-(\varepsilon_w \ln \eta)/[1 + \varepsilon_w(\ln \varepsilon_w - 1)]$
c	b/ε_w
a	$(\exp(1)/\varepsilon_w)^b$
t_η	$f_{T_{GM}} \times T_{GM}$ where $f_{T_{GM}} = 2$, $T_{GM} = \underbrace{0.5/f_a}_{\text{Source Duration}} + \underbrace{0.05R}_{\text{Path Duration}}$

Joyner (Boore and Joyner 1997). We obtained the equation (15) by curve fitting on the data in Table 3 of the mentioned study in reference (Boore and Joyner 1997).

$$A(f) = 1.274f^{0.2541} + 0.455 \tag{15}$$

Fig. 3 shows the fitness of Eq. (15) with the proposed data by Boore and Joyner. Also, $D(f)$ is given by the following equation

$$D(f) = \exp(-\pi\kappa_0 f)\left[1 + (f/f_{max})^8\right]^{-0.5} \tag{16}$$

where κ_0 and f_{max} are site diminution parameters with proposed values of 100 and 0.03 respectively in AS00 model.

3.4 The type of motion I (f)

By the filter $I(f)$, the particular type of ground motion resulting from the simulation is controlled. For different types of ground motion, $I(f)$ is given by
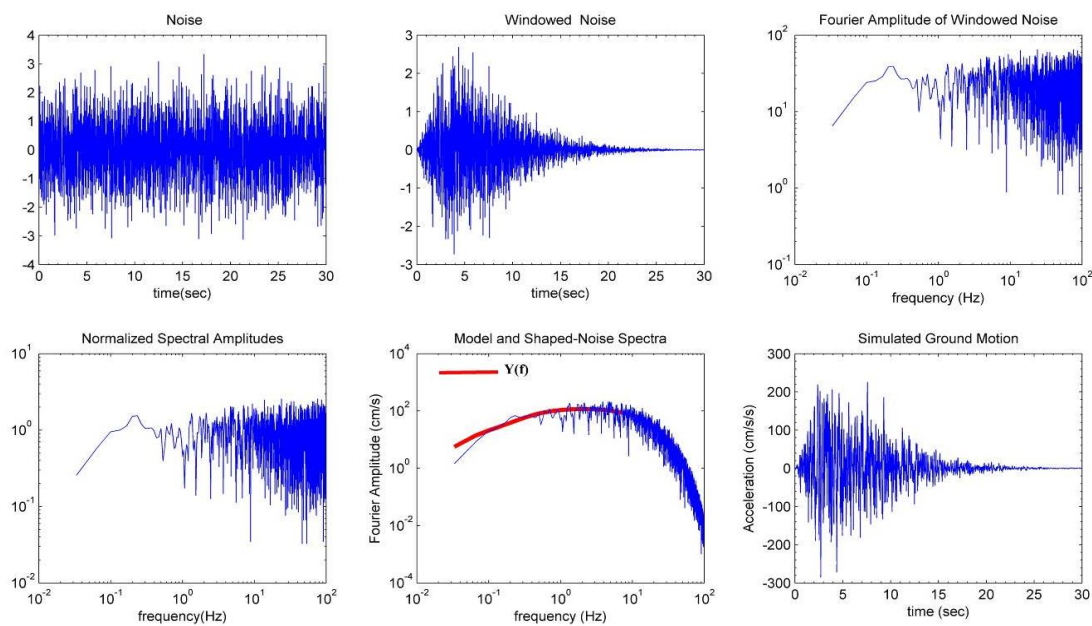
$$I(f) = (2\pi f\ i)^n \tag{17}$$

Fig. 4 Six steps of simulating ground motion using the stochastic method. M= 7 and r= 10 km and other parameters are based on AS00 model as specified.
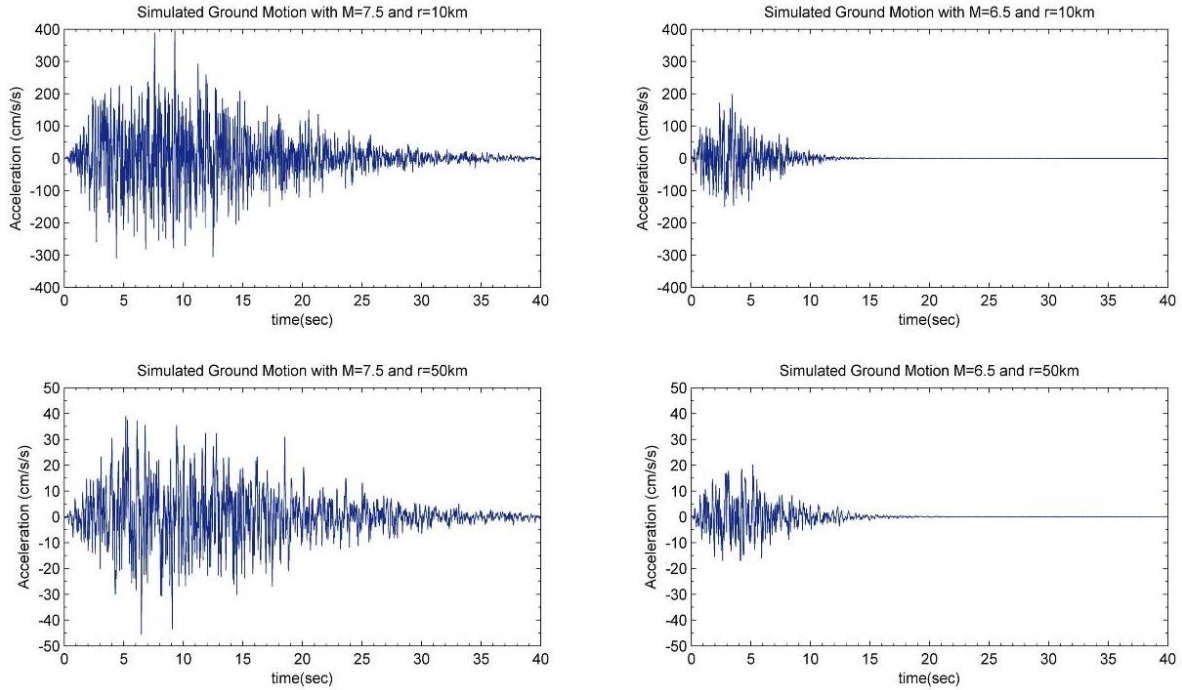
Fig. 5 Variation of acceleration time-history due to the variation of *M* and *r*

where $i = \sqrt{-1}$ and *n*=0,1 or 2 for ground displacement,velocity, or acceleration, respectively.

3.5 Simulations of acceleration time-history

By using assumptions mentioned above, the simulation procedure of artificial acceleration time histories is described as the following steps.

1. A Gaussian random white noise is generated for the given duration of motion.

2. The noise is windowed applying the envelope of acceleration time series.

3. The windowed noise is transferred to the frequency domain

4. The spectrum is normalised by the square-root of the mean square amplitude spectrum

5. The normalised spectrum is multiplied by the ground motion spectrum *Y*

6. The resulting spectrum is transformed back to the time domain

Fig. 4 graphically shows the procedure of the above steps for an earthquake with a moment magnitude *M*= 7 and closest distance to the vertical projection of the rupture surface *r*= 10 km.

The following equation gives the envelope of acceleration time series (or temporal window function)

$$w(\mathrm{t}, \varepsilon_w, \eta, t_\eta) = a(t/t_\eta)^b \exp(-c(t/t_\eta)) \qquad (18)$$

where the parameters *a*, *b*, *c*, ε_w, η, t_η are calculated using the selected parameters listed in Table 3.

For a better understanding of the effect of the earthquake parameters in the generation of artificial ground motion, variations of earthquake parameters like moment magnitude (*M*) and closest distance to the vertical

projection of the rupture surface (*r*) as the most effective parameters are studied. In Fig. 5 four plots of the acceleration time histories have been arranged for different values of *M* (7.5, 6.5) and *r* (10 km. 50 km). As shown in the figure, reduction of *M* from 7.5 to 6.5 reduced the duration and peak acceleration significantly and increase of *r* mostly results in the reduction of peak acceleration.

3.6 Generation of random variables

Even though in ground motion simulation the white noise is generated randomly, to apply entirely stochastic method, the uncertainty of the described variables should be included. Here, ten more efficient random parameters lined up as: M, r, k_0, f_a, f_b, f_{max}, ε, T_{GM}, ε_w, η.

We generated these variables randomly, and for each set, a ground motion is synthesised applying the described method.

The uncertainty of moment magnitude, *M*, is modelled by the Truncated Gutenberg–Richter relationship on the interval [M_{min}, M_{max}]=[4,5,7] with the regional seismicity factor b_M=0.9In(10). So the random generation of moment magnitude would be done by the following equation using CDF of moment magnitude

$$M = \ln(1 - U(1 - \exp(-b(M_{max} - M_{min})))) / (-b) + M_{min} \qquad (19)$$

Where *U* is uniformly distributed random variable on the interval [0.1].

The uncertainty of closest distance to the vertical projection of the rupture surface (*r*) is modelled considering fault as a line source. The cumulative density function of this variable is defined by the following equation (Der Kiureghian and Ang 1975) by assuming the closest horizontal distance between site and source is 10 kilometres

Table 4 Random variables and their distribution used in earthquake generation (Boore 2003)

Parameter	Median Value	Coefficient of Variation (C.O.V)	Distribution Type
k_0	0.03	-	Uniform on [0.02,0.04]
f_a	$10^{2.181-0.496M}$	0.2	Lognormal
f_b	$10^{2.41-0.408M}$	0.2	Lognormal
f_{max}	100	0.2	Lognormal
ε	$10^{0.605-0.255M}$	0.2	Lognormal
T_{GM}	$0.5/f_a+0.05R$	0.4	Lognormal
ε_w	0.2	0.4	Lognormal
η	0.05	0.4	Lognormal

$$F_r(\tilde{r}) = P(r < \tilde{r}) = 2\frac{\sqrt{\tilde{r}^2 - 10^2}}{L_F} \quad (20)$$

Where the length of fault projection is $L_F=10^{-3.55+0.74M}$ (Boore and Joyner 1991). From Eq. (20), r would be generated randomly by the following equation

$$r = \left[(UL_F/2)^2 + 10^2\right]^{0.5} \quad (21)$$

Other random variables have median values with the probability distribution listed in Table 4.

4. Sensitivity analysis

In reliability analysis of the supposed isolated structure besides many random variables contribute to the generation of artificial ground motions; the uncertainty of the other variables of the model should be included too. However, to decrease the number of input variables of the surrogate model, only the critical uncertain variables are considered in training and design procedure of ANN. The design variables of the FPS system (R_{FPS}, μ) would be included in input variables of ANN regardless.

Table 5 Formulas to compute S_i and S_{Ti}

S_i	Reference
$*(a) \frac{1}{N}\sum_{j=1}^{N} f(B_j)\left[f(A_{B_j}^i) - f(B_j)\right]$	(Saltelli *et al.* 2010)
$(b) V(Y) - \frac{1}{2N}\sum_{j=1}^{N}\left[f(B_j) - f(A_{B_j}^i)\right]^2$	(Jansen 1999)

S_{Ti}	Reference
$(c) \frac{1}{N}\sum_{j=1}^{N} f(A_j)\left[f(A_j) - f(A_{B_j}^i)\right]$	(Sobol 2007)
$(d) \frac{1}{2N}\sum_{j=1}^{N}\left[f(A_j) - f(A_{B_j}^i)\right]^2$	(Saltelli *et al.* 2010, Jansen 1999)

$*A_j, B_j$ and $A_{B_j}^i$ denotes the jth row of matrix A, B and A_B^i and $V(Y)$ indicates the variance of all random sample outputs

Sensitivity analysis is the study of how the uncertainty in the output of a model (numerical or otherwise) can be apportioned to different sources of uncertainty in the model input variables (Saltelli and Sobol 1995). Sample-based methods are among the most potent sensitivity analysis procedures. Variance-based sensitivity analysis as one of the efficient sample-based methods (Saltelli *et al.* 2010) can easily show each variable's portion in output uncertainty using sensitivity indices.

Consider the model as a function $Y=f(X_1, X_2, \ldots, X_K)$ where X_i ($i=1:k$) represents the ith single or set of random variables.

One of the sensitivity indices is S_i that is a normalised index. This index theoretically varies between 0 and 1 and measures the first order effect of X_i on the model output. Another popular variance-based measure is the total effect index S_{Ti} that measures the total effect, i.e., first and higher order effects of random variable X_i (Homma and Saltelli 1996, Saltelli and Tarantola 2002).

To calculate the sensitivity indices, we imagine having two independent sampling matrices A and B, with a_{ji} and b_{ji} as generic elements. The index i runs from one to k, the number of random variables, while the index j runs from

Table 6 Random variables and their distribution considered for sensitivity analysis

Representation of variable	Name	Description	Mean Value	Coefficient of Variation (C.O.V)	Distribution Type
X_1	D_C	Dimensions of square columns	400 mm	0.02	Normal (Vrouwenvelder 1997)
X_2	H_B	Height of beams	400 mm	0.02	Normal (Vrouwenvelder 1997)
X_3	W_B	Width of beams	300 mm	0.02	Normal(Vrouwenvelder 1997)
X_4	R_{FF}	Radii of curvature of FPSs	1000 mm	0.2	Normal (Vrouwenvelder 1997)
X_5	μ	Friction Coefficients of FPSs	0.11	0.1	Lognormal (Steele 2008)
X_6	DL	Dead load	$1.05 \times DL_n*$ =3675 kg/m	0.1	Normal (Ellingwood and Galambos 1983)
X_7	LL	Live load	$1 \times LL_n*$ =1500 kg/m	0.25	Extreme Value (Ellingwood and Galambos 1983)
X_8	E_C	Modulus of elasticity of concrete	$1.12 \times E_C$ =28 GPa	0.13	Lognormal (Vrouwenvelder 1997)
X_9	-	Input ground motion	-	-	Randomly generated in agreement with section 4

*DL_n and LL_n denotes the nominal dead and live loads
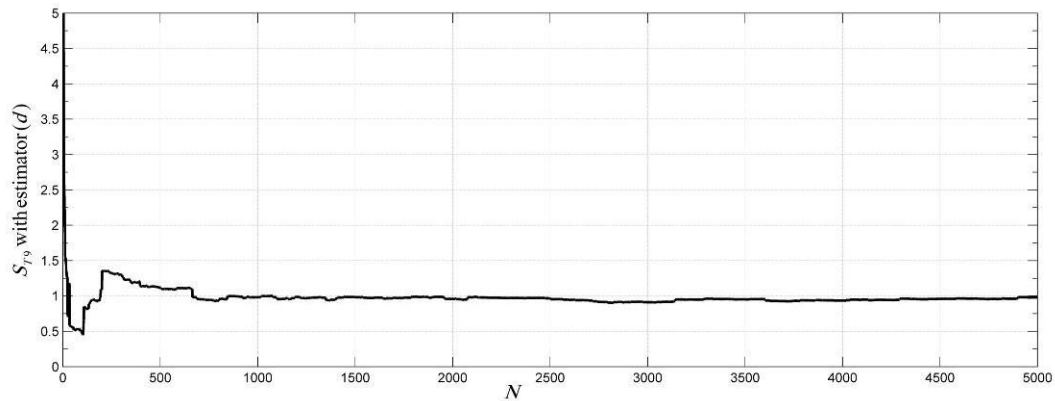
Fig. 6 Convergence of S_{T9} with estimator (d)

one to N, the number of simulations. So to create matrix A, each of random variables should randomly be generated for N times. To calculate sensitivity indices matrix A_B^i should be generated where all columns are from matrix A except the ith column which is from matrix B (Saltelli, Annoni *et al.* 2010). Now the normalised "main effect indices" S_i and "total effect indices" S_{Ti} can be calculated from the equations in Table 5.

Table 5 indicates that for each estimator (a),(b),(c) and (d) we would need ($2+k$)N simulations; $2N$ simulations for A and B matrix and kN simulations for the matrix A_B^i.

In the present study, eight random load/structural variables in addition to input ground motion are considered as random variables for sensitivity analysis. These nine single/set of variables and their distribution are introduced in Table 6. The median values for R and μ are selected based on the designed FPS system.

With N=5000 the results indicate an excellent convergence in sensitivity indices (see Fig. 6). For N=5000 it needs 55000 simulations for each estimator to be computed.

Table 7 shows the main and total effect indices (S_i and S_{Ti}) calculated with different estimators mentioned in Table 5 with N=5000.

The calculated indices with all estimators show that the first eight variables uncertainties are negligible in comparison to uncertainty in the input ground motion. So considering first eight variables as certain, would not significantly affect the reliability analysis.

5. Neural networks

Neural networks (NN) are numerical algorithms inspired in the functioning of biological neurones. McCulloch and Pitts (McCulloch and Pitts 1943) firstly introduced this concept. They proposed a mathematical model to simulate neurone behaviour (Cardoso *et al.* 2008). Nowadays NN and its recent variants (such as wavelet neural networks and wavelet support vector machine-based NN) have found its way into practical applications in many areas (Veitch 2005, Chen *et al.* 2013). Numbers of computational structures technology applications, which are heavily dependent on

Table 7 Main and total effect indices calculated with different estimators for N=5000

Variable	S_i Estimator (a)		S_i Estimator (b)		S_{Ti} Estimator (c)		S_{Ti} Estimator (d)	
	*MFA 2nd floor	MFA 3rd floor	MFA 2nd floor	MFA 3rd floor	MFA 2nd floor	MFA 3rd floor	MFA 2nd floor	MFA 3rd floor
X_1	0.0017	0.0005	0.0842	0.0383	0.0148	0.0308	0.0121	0.0215
X_2	0.0009	0.0004	0.0904	0.0422	0.0198	0.0226	0.0083	0.0172
X_3	0.0023	0.0014	0.0694	0.0721	0.0022	0.0105	0.0104	0.0158
X_4	0.0007	0.0023	0.0830	0.0694	0.0094	0.0083	0.0070	0.0116
X_5	0.0051	0.0022	0.0569	0.0641	0.0057	0.0098	0.0337	0.0289
X_6	0.0025	0.0013	0.1062	0.0482	0.0517	0.0234	0.0228	0.0257
X_7	0.0004	0.0054	0.0655	0.0495	0.0012	0.0117	0.0150	0.0194
X_8	0.0002	0.0014	0.0623	0.0749	0.0063	0.0058	0.0114	0.0205
X_9	0.7755	1.0244	0.9662	0.9447	1.0408	0.9801	0.9299	1.0126

*Maximum Floor Acceleration

extensive computer resources, have been investigated, showing the range of application of neural network capabilities. The basic idea of applying NN here is to use it as the RSM as an evaluation of the limit state in MCS. The significant advantage of a trained NN over the conventional numerical process is that results can be produced in a few clock cycles, requiring orders of magnitude less computational effort than the conventional computational process. More detailed introduction to NN may be found in (Schmidhuber 2015).

5.1 The NN training and assumptions

Herein, the efficiency of the proposed method of application of the NN is investigated to predict the maximum structural responses in the context of reliability analysis. This objective comprises the following tasks:
(i) Select the proper training set.
(ii) Find suitable network architecture.
(iii) Determine the appropriate values of characteristic parameters.
The Back Propagation (BP) algorithm according to Levenberg-Marquardt optimisation (Wilamowski, Iplikci *et al.* 2001) is used as the learning algorithm that updates
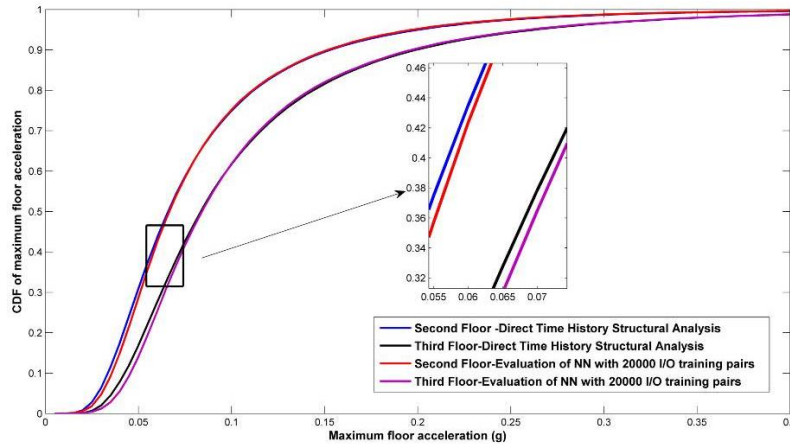
Fig. 7 CDF of maximum floor acceleration for second and third floor

weight and bias states.

The number of neurones to be employed in the hidden layers is not known in advance and usually, is estimated by trial and error.However, the number of 100 hidden layers shows good results in output estimations.

The comparison of the predicted results with the target results computed using the root mean square (RMS), controls the convergence of the training process.

For validation and testing, 30% of I/O training pairs are randomly extracted (each one 15%), and the training is done with the remained 70% I/O training pairs.

The input variables for the NN are the design variables of FPS in addition to parameters of random motion generation regarding the results of sensitivity analysis, and the outputs are maximum floor accelerations of the second and third floors of the building.

After the selection of the suitable NN architecture and the performance of the training procedure, the network is used to produce predictions of limit state function corresponding to different values of the input variables. The results are then processed using MCS to calculate the probability of failure P_f.

6. Results

Herein due to the results of the sensitivity analysis, we only exerted the uncertainty of ground motion in the model. We considered the ten most important variables of the ground motion generation $(M,r,k_0,f_a,f_b,f_{max},\varepsilon,T_{GM},\varepsilon_w,\eta)$ as uncertain variables. These variables are previously mentioned in section 3. Other two design variables are R_{FPS}, μ that are considered as uniformly distributed on $[0.1_m,10_m]$ and $[0.02,0.2]$ respectively. So the surrogate model would have twelve input variables that are: $[R_{FPS},\mu,M,r,k_0,f_a,f_b,f_{max},\varepsilon,T_{GM},\varepsilon_w,\eta]$.

The Monte Carlo simulation approach consists of drawing samples of variables according to their probability density functions and then feeding them into the mathematical model $g(X)$. The samples thus obtained would give all the probabilistic characteristics of the structural response as a random variable. However, for calculation of the probability of failure if N_f is the number of simulation cycles when $g(X)$ is less than zero then $P_f=N_f/N$ where N is the total number of simulations.

To have data for validation procedure, at first 100,000 sets of the ten uncertain random variables of the ground motion model were generated as input variables of the structural model. Then the maximum responses of the structure for these sets were obtained using dynamic time-history analysis of the structural model considering μ=0.11 and R_{FPS}=1 m as the design variables of FPS. Afterwards, cumulative distribution functions (CDF) of the maximum floor accelerations (MFA) of the equipped stories were obtained. Fig. 7 shows the CDF of MFA for both equipped floors. From this figure, it can be concluded that the floor accelerations do not pass the threshold of 0.4 g.

For training data, 200,000 sets of the twelve random variables including $[R_{FPS},\mu,M,r,k_0,f_a,f_b,f_{max},\varepsilon,T_{GM},\varepsilon_w,\eta]$, were generated as input variables of the structural model. Then the maximum responses of the structure for these sets were obtained using dynamic time-history analysis of the structural model. For design procedure of ANNs, these I/O pairs were selected to train the NNs. For each maximum response of the equipped floors, a specific NN was designed and trained. Then 100,000 new sets of the ten uncertain random variables of the ground motion model were generated, and Monte Carlo simulations were done using designed NNs instead of the dynamic structural time-history analysis. For the first two input variables of NNs, we again supposed μ=0.11 and R_{FPS}=1 m in all Monte Carlo simulations. This time the CDF of MFA was obtained from the evaluations of designed NNs. Fig. 7 shows the results of NNs estimations in comparison to direct structural time-history analysis.

Considering Eqs. (1) and (2), the probability of failure for all acceleration thresholds can be obtained from the CDF of the MFA using the following equation

$$\begin{aligned} P_f &= P\left[g(X) \le 0\right] = P\left[MFA \ge a_t\right] \\ &= 1 - P\left[MFA < a_t\right] = 1 - CDF(MFA) \end{aligned} \quad (22)$$

Fig. 8 shows the obtained probability of failures for all acceleration thresholds (a_t) using NN estimations of limit state in comparison to direct time-history analysis of structure. The figure indicates that the estimates of the NNs
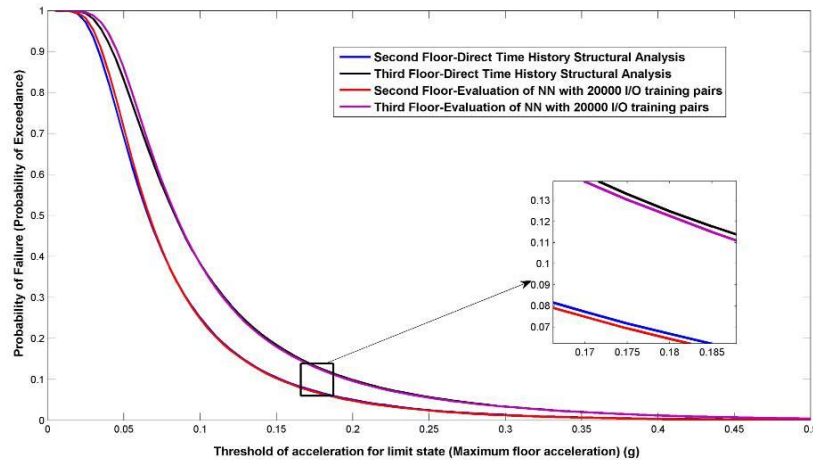
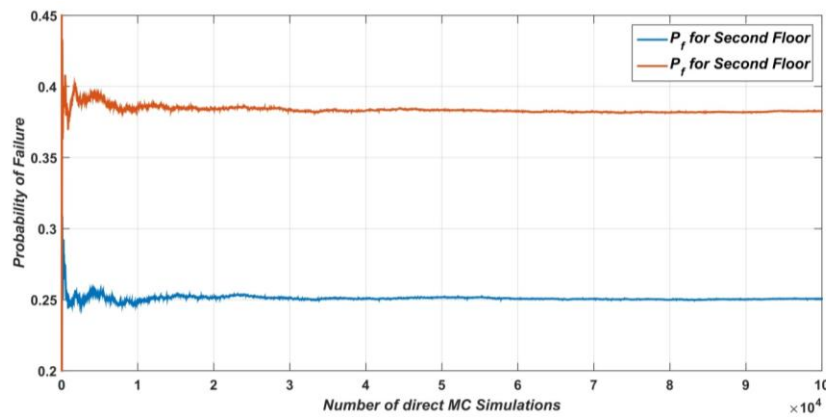Fig. 8 Probability of failure considering different acceleration thresholds for second and third floors

Fig. 9 Convergence of Probability of failure using time history analysis and direct MCS

Table 8 Probability of failure computed using different generated NN by various numbers of I/O training pairs and their error into results of 100,000 direct time-history structural analysis simulations (P_f)

	Number of I/O training Pairs	1000	2000	5000	10000	20000	50000	100000	200000
Second Floor	Probability of failure using neural network (P_f^{NN})	0.33575	0.32432	0.31523	0.27475	0.24789	0.25307	0.25167	0.25041
	$e(\%) = \dfrac{\left|P_f^{NN} - P_f\right|}{P_f} \times 100$	33.95	29.39	25.76	9.61	1.10	0.97	0.41	0.09
Third Floor	Probability of failure using neural network (P_f^{NN})	0.63222	0.44963	0.33524	0.41239	0.40907	0.39275	0.37501	0.38205
	$e(\%) = \dfrac{\left|P_f^{NN} - P_f\right|}{P_f} \times 100$	65.27	17.54	12.36	7.81	6.94	2.67	1.97	0.12

made such close results, especially for higher acceleration thresholds.

Also for a better comparison, several NNs were designed with the various numbers of I/O training pairs. Then for a specific acceleration threshold a_t=100 milli-g, the probability of failure was computed using estimations of these NNs. The convergence of the P_f for second and third floors using time-history analysis and direct MCS are shown in Fig. 9.

The number of direct Monte Carlo simulations is the same when using either NNs or direct time-history analysis (100,000 Monte Carlo simulations). Table 8 shows the results.

According to the results and the errors (e%) showed in Table 8, the probability of failure obtained using NNs exhibits excellent compatibility with the ones achieved by structural time-history analysis for above 10000 I/O training pairs. So if a lesser accuracy of P_f is acceptable, the 200000 I/O training pairs can even be decreased to the 10000 I/O pairs.

It took about 121946 seconds for a specific computer to run 100,000 simulations based on the direct time-history analysis of the structure. This time decreases to just 0.817 seconds with the same computer using the estimations of trained NN. So the computation cost for Monte Carlo simulations can be significantly reduced using the surrogate

model.

Although the reliability analysis considering an FPS with specific properties (R, μ) does not impose high calculation cost, in the optimal reliability-based design of an isolated structure, the failure probability should be calculated for several times due to the properties variation of the isolation system. This fact can show the efficiency of the proposed model.

7. Conclusions

In this paper, we presented an efficient method to reduce the cost of reliability analysis of a structure isolated with FPS. At first, a unique sensitivity analysis was conducted to decrease the number of uncertain variables. The sensitivity procedure leads to a reduction of computation cost for training and design process of NNs. Sensitivity analysis showed that the uncertainty of all variables is negligible in comparison to the randomness of input ground motion.

Then the reliability of the structure was computed using the estimations of the limit state by the designed NNs to show the efficiency of this method. The limit state was defined based on the maximum response of the structure floors.

At last, we compare the results of the direct time-history analysis with the ones obtained from the estimations of NN.

The probability of failure that obtained using NNs shows excellent compatibility with the ones achieved by structural time-history analysis. The results would be striking considering that the required time for 100,000 Monte-Carlo simulations using NNs is less than even a single dynamic time-history analysis of the structure. It would significantly help the computation process when the reliability of the structure should be evaluated several times for example in the optimal reliability-based design of structures.

References

Adeli, H. and Jiang, X. (2006), "Dynamic fuzzy wavelet neural network model for structural system identification", *J. Struct. Eng*., **132**(1), 102-111.

Alhan, C. and Gavin, H.P. (2005), "Reliability of base isolation for the protection of critical equipment from earthquake hazards", *Eng. Struct*., **27**(9), 1435-1449.

Atkinson, G.M. and Silva, W. (2000), "Stochastic modeling of California ground motions", *Bull. Seismol. Soc. Am*., **90**(2), 255-274.

Ayyub, B.M. and McCuen, R.H. (2011), *Probability, Statistics, and Reliability for Engineers and Scientists*, CRC press

Boore, D.M. (2003), "Simulation of ground motion using the stochastic method", *Pure Appl. Geophys*., **160**(3-4), 635-676.

Boore, D.M. and Joyner, W.B. (1991), "Estimation of ground motion at deep-soil sites in eastern North America", *Bull. Seismol. Soc. Am*., **81**(6), 2167-2185.

Boore, D.M. and Joyner, W.B. (1997), "Site amplifications for generic rock sites", *Bull. Seismol. Soc. Am*., **87**(2), 327-341.

Bucher, C. (2009), *Computational Analysis of Randomness in Structural Mechanics: Structures and Infrastructures Book Series*, CRC Press

Bucher, C. (2015). "Analysis and design of sliding isolation

pendulum systems", *IABSE Symposium Report*.

Cardoso, J.B., de Almeida, J.R., Dias, J.M. and Coelho, P.G. (2008), "Structural reliability analysis using Monte Carlo simulation and neural networks", *Adv. Eng. Softw*., **39**(6), 505-513.

Castaldo, P. and Tubaldi, E. (2015), "Influence of FPS bearing properties on the seismic performance of base-isolated structures", *Earthq. Eng. Struct. Dyn*., **44**(15), 2817-2836

Chen, F., Tang, B. and Chen, R. (2013), "A novel fault diagnosis model for gearbox based on wavelet support vector machine with immune genetic algorithm", *Measur*., **46**(1), 220-232.

Chen, J., Liu, W., Peng, Y. and Li, J. (2007), "Stochastic seismic response and reliability analysis of base-isolated structures", *J. Earthq. Eng*., **11**(6), 903-924.

Constantinou, M., Mokha, A. and Reinhorn, A. (1990), "Teflon bearings in base isolation II: Modeling", *J. Struct. Eng*., **116**(2), 455-474.

Constantinou, M. and Papageorgiou, A. (1990), "Stochastic response of practical sliding isolation systems", *Prob. Eng. Mech*., **5**(1), 27-34.

Dai, H., Zhang, H. and Wang, W. (2015), "A Multiwavelet Neural Network-Based Response Surface Method for Structural Reliability Analysis", *Comput. Aid. Civil Infrastr. Eng*., **30**(2), 151-162.

Der Kiureghian, A. and Ang, A.S. (1975), "A line source model for seismic risk analysis", University of Illinois Engineering Experiment Station. College of Engineering. University of Illinois at Urbana-Champaign.

Desai, K.M., Survase, S.A., Saudagar, P.S., Lele, S. and Singhal, R.S. (2008), "Comparison of artificial neural network (ANN) and response surface methodology (RSM) in fermentation media optimization: case study of fermentative production of scleroglucan", *Biochem. Eng. J*., **41**(3), 266-273.

Ellingwood, B. and Galambos, T.V. (1983), "Probability-based criteria for structural design", *Struct. Saf*., **1**(1), 15-26.

Enevoldsen, I. and Sørensen, J.D. (1994), "Reliability-based optimization in structural engineering", *Struct. Saf*., **15**(3), 169-196.

Farooq Anjum, M., Tasadduq, I. and Al-Sultan, K. (1997), "Response surface methodology: A neural network approach", *Eur. J. Operat. Res*., **101**(1), 65-73.

Gomes, H.M. and Awruch, A.M. (2004), "Comparison of response surface and neural network with other methods for structural reliability analysis", *Struct. Saf*., **26**(1), 49-67.

Gosavi, A. (2003), *Simulation-based Optimization: Parametric Optimization Techniques and Reinforcement Learning*, Springer

Gosavi, A. (2014), *Simulation-based Optimization: Parametric Optimization Techniques and Reinforcement Learning*, Springer

Homma, T. and Saltelli, A. (1996), "Importance measures in global sensitivity analysis of nonlinear models", *Reliab. Eng. Syst. Saf*., **52**(1), 1-17.

Huang, T.L. and Ren, W.X. (2011). "Dynamic reliability-based seismic optimal design of base-isolated structures", *Adv. Mater. Res*., **243**, 3765-3769

Iman, R.L. (2008), *Latin Hypercube Sampling*, Wiley Online Library

Jansen, M.J. (1999), "Analysis of variance designs for model output", *Comput. Phys. Commun*., **117**(1), 35-43.

Jia, G., Gidaris, I., Taflanidis, A.A. and Mavroeidis, G.P. (2014), "Reliability-based assessment/design of floor isolation systems", *Eng. Struct*., **78**, 41-56.

Kerh, T. and Ting, S. (2005), "Neural network estimation of ground peak acceleration at stations along Taiwan high-speed rail system", *Eng. Appl. Artif. Intell*., **18**(7), 857-866.

Lin, Y.-K. and Cai, G.-Q. (1995), *Probabilistic Structural Dynamics: Advanced Theory and Applications*, McGraw-Hill New York

Liu, Y.Y., Ju, Y.F., Duan, C.D. and Zhao, X.F. (2011), "Structure damage diagnosis using neural network and feature fusion", *Eng. Appl. Artif. Intell.*, **24**(1), 87-92.

Lomiento, G., Bonessio, N. and Benzoni, G. (2013), "Friction Model for Sliding Bearings under Seismic Excitation", *J. Earthq. Eng.*, **17**(8), 1162-1191.

Mayes, R.L. and Naeim, F. (2001), *Design of Structures with Seismic Isolation*, Springer

McCulloch, W.S. and Pitts, W. (1943), "A logical calculus of the ideas immanent in nervous activity", *Bull. Math. Biophys.*, **5**(4), 115-133.

Moeindarbari, H., Malekzadeh, M. and Taghikhany, T. (2014), "Probabilistic analysis of seismically isolated elevated liquid storage tank using multi-phase friction bearing", *Earthq. Struct.*, **6**(1), 111-125.

Moeindarbari, H. and Taghikhany, T. (2014), "Seismic optimum design of triple friction pendulum bearing subjected to near-fault pulse-like ground motions", *Struct. Multidisc. Optim.*, **50**(4), 1-16.

Mokha, A., Constantinou, M. and Reinhorn, A. (1990), "Teflon bearings in base isolation I: Testing", *J. Struct. Eng.*, **116**(2), 438-454.

Palazzo, B., Castaldo, P. and Della Vecchia, P. (2014). "Seismic reliability analysis of base-isolated structures with friction pendulum system", *Environmental Energy and Structural Monitoring Systems (EESMS), 2014 IEEE Workshop on*.

Papadrakakis, M. and Lagaros, N.D. (2002), "Reliability-based structural optimization using neural networks and Monte Carlo simulation", *Comput. Meth. Appl. Mech. Eng.*, **191**(32), 3491-3507.

Papadrakakis, M., Tsompanakis, Y., Lagaros, N.D. and Fragiadakis, M. (2004), "Reliability based optimization of steel frames under seismic loading conditions using evolutionary computation", *J. Theor. Appl. Mech.*, **42**(3), 585-608.

Pourgharibshahi, A. and Taghikhany, T. (2012), "Reliability-based assessment of deteriorating steel moment resisting frames", *J. Constr. Steel Res.*, **71**, 219-230.

Saltelli, A., Annoni, P., Azzini, I., Campolongo, F., Ratto, M. and Tarantola, S. (2010), "Variance based sensitivity analysis of model output. Design and estimator for the total sensitivity index", *Comput. Phys. Commun.*, **181**(2), 259-270.

Saltelli, A. and Sobol, I.M. (1995), "About the use of rank transformation in sensitivity analysis of model output", *Reliab. Eng. Syst. Saf.*, **50**(3), 225-239.

Saltelli, A. and Tarantola, S. (2002), "On the relative importance of input factors in mathematical models: safety assessment for nuclear waste disposal", *J. Am. Stat. Assoc.*, **97**(459), 702-709.

Schmidhuber, J. (2015), "Deep learning in neural networks: An overview", *Neur. Network.*, **61** 85-117.

Shahbazi, P. and Taghikhany, T. (2017), "Sensitivity analysis of variable curvature friction pendulum isolator under near-fault ground motions", *Smart Struct. Syst.*, **20**(1), 23-33.

Sobol', I.Y.M. (2007), "Global sensitivity indices for the investigation of nonlinear mathematical models", *Matematicheskoe Modelirovanie*, **19**(11), 23-24.

Steele, C. (2008), "Use of the lognormal distribution for the coefficients of friction and wear", *Reliab. Eng. Syst. Saf.*, **93**(10), 1574-1576.

Su, L. and Ahmadi, G. (1988), "Response of frictional base isolation systems to horizontal-vertical random earthquake excitations", *Prob. Eng. Mech.*, **3**(1), 12-21.

Taflanidis, A.A. and Jia, G. (2011), "A simulation-based framework for risk assessment and probabilistic sensitivity analysis of base-isolated structures", *Earthq. Eng. Struct. Dyn.*, **40**(14), 1629-1651.

Veitch, D. (2005), "Wavelet Neural Networks and their application in the study of dynamical systems", Department of Mathematics University of York, UK.

Vrouwenvelder, T. (1997), "The JCSS probabilistic model code", *Struct. Saf.*, **19**(3), 245-251.

Wilamowski, B.M., Iplikci, S., Kaynak, O. and Efe, M.Ö. (2001). "An algorithm for fast convergence in training neural networks", *Proceedings of the International Joint Conference on Neural Networks*.

Zayas, V.A., Low, S.S. and Mahin, S.A. (1990), "A simple pendulum technique for achieving seismic isolation", *Earthq. Spectra.*, **6**(2), 317-333.

Zou, X.K., Wang, Q., Li, G. and Chan, C.M. (2010), "Integrated reliability-based seismic drift design optimization of base-isolated concrete buildings", *J. Struct. Eng.*, **136**(10), 1282-1295.

CC